Analysis of Liver Cancer Cell Lines Identifies Agents With Likely Efficacy Against Hepatocellular Carcinoma and Markers of Response

Stefano Caruso, Anna-Line Calatayud, Jill Pilet, Tiziana La Bella, Samia Rekik, Sandrine Imbeaud, Eric Letouzé, Léa Meunier, Quentin Bayard, Nataliya Rohr-Udilova, et al.

Accepted Manuscript

Analysis of Liver Cancer Cell Lines Identifies Agents With Likely Efficacy Against Hepatocellular Carcinoma and Markers of Response

Stefano Caruso, Anna-Line Calatayud, Jill Pilet, Tiziana La Bella, Samia Rekik, Sandrine Imbeaud, Eric Letouzé, Léa Meunier, Quentin Bayard, Nataliya Rohr-Udilova, Camille Péneau, Bettina Grasl-Kraupp, Leanne de Koning, Bérengère Ouine, Paulette Bioulac-Sage, Gabrielle Couchy, Julien Calderaro, Jean-Charles Nault, Jessica Zucman-Rossi, Sandra Rebouissou

PII: S0016-5085(19)36771-X
DOI: https://doi.org/10.1053/j.gastro.2019.05.001
Reference: YGAST 62635

To appear in: *Gastroenterology*
Accepted Date: 1 May 2019

Please cite this article as: Caruso S, Calatayud A-L, Pilet J, La Bella T, Rekik S, Imbeaud S, Letouzé E, Meunier L, Bayard Q, Rohr-Udilova N, Péneau C, Grasl-Kraupp B, de Koning L, Ouine B, Bioulac-Sage P, Couchy G, Calderaro J, Nault J-C, Zucman-Rossi J, Rebouissou S, Analysis of Liver Cancer Cell Lines Identifies Agents With Likely Efficacy Against Hepatocellular Carcinoma and Markers of Response, *Gastroenterology* (2019), doi: https://doi.org/10.1053/j.gastro.2019.05.001.

Molecular characterization

- Mutations/CNA [WES]
- Transcriptome [RNA-seq]
- miRNome [miRNA seq]
- 126 proteins [RPPA]

Pharmacological profiling

31 drugs
approved/
clinical trials

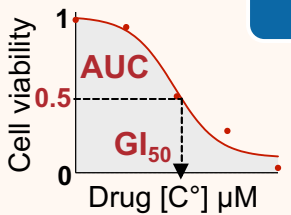

Liver Cancer Cell Lines

n=34

Transcriptome subgroups	CL1	CL2	CL3
Differentiation	Hepatoblast-like	Mixed epithelial -mesenchymal	Mesenchymal-like
Main molecular features	*TERT* promoter, *TP53*, *AXIN1*, *TSC1/TSC2* mut 11q13 amplification (*FGF19* and *CCND1*)		
	Progenitor features: *IGF2*, *AFP*, *EPCAM*+	Wnt-TGFß signaling Phospho-ß-catenin S675	
	CK19+		
Drug/ Biomarker pairs	Linsitinib		
	Sorafenib + MK2206		
	Sorafenib + MEK1/2 inhibitors		
	Trametinib/*FGF19* ampli		
	FGFR4 inhibitors/*FGF19* ampli		
	Dasatinib/CK19		
	Alisertib/*TP53* mut		
	Rapamycin/*TSC1-TSC2* mut		
	MET inhibitors: **Cabozantinib**/*MET* ampli		
	Alvespimycin,Tanespimicyn/NQO1		

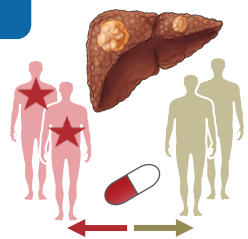

Analysis of Liver Cancer Cell Lines Identifies Agents With Likely Efficacy Against Hepatocellular Carcinoma and Markers of Response

Short title: HCC cell lines to predict drug response

Authors

Stefano Caruso*[1,2], Anna-Line Calatayud*[1,2], Jill Pilet*[1,2], Tiziana La Bella[1,2], Samia Rekik[1,2], Sandrine Imbeaud[1,2], Eric Letouzé[1,2], Léa Meunier[1,2], Quentin Bayard[1,2], Nataliya Rohr-Udilova[3], Camille Péneau[1,2], Bettina Grasl-Kraupp[4], Leanne de Koning[5], Bérengère Ouine[5], Paulette Bioulac-Sage[6,7], Gabrielle Couchy[1,2], Julien Calderaro[8], Jean-Charles Nault[1,2,9,10], Jessica Zucman-Rossi[§1,2,11#], Sandra Rebouissou[§1,2#].

Institutions

[1]Centre de Recherche des Cordeliers, Sorbonne Universités, Inserm, UMRS-1138, F-75006 Paris, France;

[2]Functional Genomics of Solid Tumors, USPC, Université Paris Descartes, Université Paris Diderot, Université Paris 13, Labex Immuno-Oncology, équipe labellisée Ligue Contre le Cancer, F-75000 Paris, France;

[3]Division of Gastroenterology and Hepatology, Clinic of Internal, Medicine III, Medical University of Vienna, Vienna, Austria;

[4]Department of Medicine I, Division: Institute of Cancer Research, Comprehensive Cancer Center, Medical University of Vienna, Vienna, Austria;

[5]RPPA platform, Curie Institute, PSL research university, Paris, France;

[6]Bariton INSERM, UMR-1053, Bordeaux, France;

[7]Department of Pathology, Pellegrin Hospital, Hospital of Bordeaux, Bordeaux, France;

[8]Anathomopathology Department, Henri Mondor Hospital, Créteil; University of Paris Est Créteil, Inserm U955, Team 18, Mondor Institute of Biomedical Research, France;

[9]Liver unit, Jean Verdier Hospital, University Hospitals Paris-Seine-Saint-Denis, AP-HP, Bondy, France;

[10]Training and Research Unit of Health Medicine and Human Biology, University of Paris 13, Community of Universities and Institutions Sorbonne Paris Cité, Paris, France;

[11]European Hospital Georges Pompidou, AP-HP, F-75015, Paris, France

* These authors contributed equally to this work

§ These authors contributed equally to this work

Grant supports: This work was supported by Inserm, the Association Française pour l'Etude du Foie (AFEF). The team is supported by the Ligue Nationale Contre le Cancer (Equipe Labellisée), Labex OncoImmunology (Investissement d'Avenir), the Fondation Bettencourt-Schueller (coup d'élan Award), the Ligue Contre le Cancer Comité de Paris (Duquesne award) and the Fondation pour la Recherche Médicale (Raymond Rosen award). SC is supported by a funding from Labex OncoImunology and CARPEM. ALC, LM and QB are supported by a fellowship from the Ministère de l'Education Nationale de la Recherche et de Technologie (MENRT) and JP, SRek and CP received a fellowship from the Fondation pour la Recherche Médicale (FRM), Association pour la Recherche sur le Cancer (ARC) and ANRS, respectively.

Abbreviations: LCCL: liver cancer cell lines, HCC: hepatocellular carcinoma, RT-PCR: reverse transcriptase polymerase chain reaction, RPPA: reverse phase protein array, WES: whole exome sequencing, CNA: copy number alterations, EN: elastic net, EMT: epithelial-mesenchymal transition, SD: standard deviation, TSG: tumor suppressor gene

#Corresponding Authors:

Sandra Rebouissou, PhD

Inserm UMRS-1138, Functional Genomics of Solid Tumors

27 rue Juliette Dodu

75010 Paris, France

TEL: +33 1 72 63 93 55

Email: sandra.rebouissou@inserm.fr

Jessica Zucman-Rossi, MD, PhD

Inserm UMRS-1138, Functional Genomics of Solid Tumors

27 rue Juliette Dodu

75010 Paris, France

TEL: +33 1 72 63 93 58

Email: jessica.zucman-rossi@inserm.fr

Disclosures: The authors disclose no conflicts.

Accession codes: The sequencing data reported in this study (WES, RNA-sequencing and miRNA-sequencing) have been deposited to the EGA (European Genome-phenome Archive) database and are available through the accession number [EGAS00001003536].

All the molecular and drug sensitivity data are available at: http://lccl.zucmanlab.com

Writing Assistance: no writing assistance

Author Contributions:

Study concept and design: SR, JZR

Acquisition of data: ALC, JP, SRek, TLB, CP, LDK, BO, GC, JCN

Analysis and interpretation of data: SC, SI, EL, LM, QB

Drafting of the manuscript: SC, ALC, SR, JZR

Collection of samples: NRU, BGK, PBS, JC, JCN

Study supervision: SR, JZR

Revision of the manuscript and approval of the final version of the manuscript: ALL

Acknowledgments: We thank Philippe Merle and Fabien Zoulim for providing the HepaRG cell line. We would like also to thank Sabine Rajkumar, Caroline Lecerf, Floriane Bard and Audrey Criqui for acquisition of RPPA data. We warmly thank Aurélien de Reyniès for providing the R-package for the transcriptomic prediction of Hoshida's and Boyault's HCC molecular subclasses. We are grateful to Frédéric Soysouvanh for help in drug screening. We thank Stephen Miller from Blueprint Medicines for providing us the FGFR4 inhibitor BLU9931. We thank all the clinician surgeons and pathologists who have participated to this work: Jean Saric, Christophe Laurent, Laurence Chiche, Brigitte Le Bail, Claire Castain (CHU Bordeaux), Alexis Laurent, Daniel Cherqui, Daniel Azoulay (CHU Henri Mondor, Créteil, APHP), Marianne Ziol, Nathalie Ganne-Carrié and Pierre Nahon (Jean Verdier Hospital, Bondy, APHP). We also thank the Réseau national CRB Foie (BB-0033-0085), the tumor banks of CHU Bordeaux (BB-0033-00036), Jean Verdier Hospital (APHP) and CHU

Henri Mondor (APHP) for contributing to the tissue collection. We warmly thank Yannick Ladeiro, Giuseppe Maltese and Codebase for their very important support during the website building process.

ABSTRACT

Background and aims: Hepatocellular carcinomas (HCCs) are heterogeneous aggressive tumors with low rates of response to treatment at advanced stages. We screened a large panel of liver cancer cell lines (LCCLs) to identify agents that might be effective against HCC and markers of therapeutic response.

Methods: We performed whole-exome RNA and microRNA sequencing and quantification of 126 proteins in 34 LCCLs. We screened 31 anti-cancer agents for their ability to decrease cell viability. We compared genetic, RNA, and protein profiles of LCCLs with those of primary HCC samples and searched for markers of response.

Results: The protein and RNA signatures of the LCCLs were similar to those of the proliferation class of HCC, which is the most aggressive tumor type. Cell lines with alterations in genes encoding members of the Ras–MAPK signaling pathway and that required FGF19 signaling via FGFR4 for survival were more sensitive to trametinib than to FGFR4 inhibitors. Amplification of *FGF19* resulted in increased activity of FGF19 only in tumor cells that kept a gene expression pattern of hepatocyte differentiation. We identified single agents and combinations of agents that reduced viability of cells with features of the progenitor subclass of HCC. LCCLs with inactivating mutations in *TSC1* and *TSC2* were sensitive to the mTOR inhibitor rapamycin, and cells with inactivating mutation in *TP53* were sensitive to the AURKA inhibitor alisertib. Amplification of *MET* was associated with hypersensitivity to cabozantinib and the combination of sorafenib and inhibitors of MEK1 and MEK2 had a synergistic anti-proliferative effect.

Conclusion: LCCLs can be screened for drugs and agents that might be effective for treatment of HCC. We identified genetic alterations and gene expression patterns associated with response to these agents. This information might be used to select patients for clinical trials.

Keywords: MEK inhibitor, liver tumor, biomarker, response to therapy

INTRODUCTION

Hepatocellular carcinoma (HCC) is an aggressive malignancy with few therapeutic options at advanced stages. Since 2008, sorafenib was the only systemic therapy approved in first-line for unresectable HCC.[1] Recently, four new agents demonstrated significant survival advantage in phase 3 clinical trials in first-line (lenvatinib)[2] and second-line (regorafenib, cabozantinib and ramucirumab)[3–5] and the FDA has granted an accelerated approval to nivolumab for HCC patients after sorafenib failure.[6] However, all these compounds provide only limited benefit in terms of survival (2-3 months) with low response rates and high inter-individual variability. These observations could be related to the high degree of molecular complexity and diversity of HCC, which usually play a critical role in determining variable tumor response of patients to treatment. Biological markers are increasingly used in clinical oncology for diagnosis, prognosis, and therapeutic decision-making and have helped to improve patient outcomes in various cancers. In HCC, there are currently no validated predictive molecular markers available for the most effective systemic treatments.

Human tumor-derived cell lines have been widely used as models for studying cancer biology. They are very useful to understand mechanisms that drive resistance and sensitivity to anti-cancer compounds, in particular when access to tissue samples is limited as in HCC for which non-invasive imaging has replaced biopsy for diagnosis.[7] Over the past decade several large-scale pharmacogenomics studies in cancer cell lines including NCI-60, CCLE (Cancer Cell Line Encyclopedia) and GDSC (Genomics of Drug Sensitivity in Cancer) have proven their value for biomarker discovery as well as to uncover mechanism of drug action and determine molecular contexts associated with specific tumor vulnerabilities.[8–10] Although these programs have provided a wealth of publically available data for the scientific community, HCC cell lines were under-represented in these different datasets. Given the molecular heterogeneity of HCC, the analysis of a large panel of cell lines recapitulating HCC

diversity may be more informative and may help to better translate *in vitro* pharmacogenomics findings into clinical application.

The goal of this study was to identify molecular features that are predictive of drug sensitivity in HCC, focusing mainly on candidate drugs already approved or in clinical development and targeting key pathways involved in hepatocarcinogenesis. To this aim, we used a collection of 34 human liver cancer derived cell lines characterized extensively at the genomic, transcriptomic and protein level. Our purpose was to understand pharmacological responses in the light of molecular profiles across the whole panel of liver cancer cell lines in order to identify 1) new potential attractive drugs in the treatment of HCC 2) molecular markers predicting their sensitivity.

MATERIALS AND METHODS

Cell lines

The 34 Liver cancer cell lines (LCCL) were collected from public repositories or collaborations and grown in monolayers in quite similar conditions, at 37°C in a humidified 5% CO_2 incubator (Supplementary Table 1). Cell line identity was verified by whole exome sequencing (WES), BEL7402 and SMMC7721 cell lines were excluded because contaminated by HeLa cells as well as SK-HEP-1 that has an endothelial origin.[11]

Identification of putative somatic variants and copy number analysis

Identification of gene mutations and copy number alterations (CNA) was performed by WES (Supplementary Material). *TERT* promoter and exon 1 of *ARID1A* were screened by Sanger sequencing because of low coverage in WES, as previously described.[12]

Selection of cancer driver genes in primary HCC tumors and comparison with LCCL

We selected 72 HCC cancer driver genes from 5 HCC publically available datasets to compare their alteration frequency between HCC and LCCL (Supplementary Table 2A). See the Supplementary Material for detailed description.

Mutational signature analysis

We used the *Palimpsest* R package to extract mutational signatures from WES data using the open-source R package on Github: https://github.com/FunGeST/Palimpsest.[13]

RNA-sequencing

Total mRNA extraction was performed for the 34 LCCL using RNeasy mini kit (Qiagen) and quality was checked. 5 μg of total RNA was used for sequencing (Supplementary Material).

Gene fusion prediction and HBV integration

Fusions detected by TopHat2 (--fusion-search --fusion-min-dist 2000 --fusion-anchor-length 13 --fusion-ignore-chromosomes chrM) were filtered using the TopHatFusion-post algorithm. We kept only fusions validated by BLAST and with at least 10 split-reads or pairs of reads spanning the fusion event, and we removed fusions identified at least twice in a cohort of 36 normal liver samples. HBV insertions were screened as described in the Supplementary Material.

Transcriptome analysis

Consensus clustering was performed with Bioconductor *ConsensusClusterPlus* package. Principal component analysis using the first 3 components was also generated.

The Bioconductor *DESeq2* package was used to detect differentially expressed genes between the LCCL transcriptomic subgroups. Detailed analysis as well as Hoshida's and Boyault's prediction subclasses are described in the Supplementary Material.

miRNA profiling

Total miRNA extraction from 34 LCCL was performed using TRIzol reagent (Thermo Fisher Scientific, Carlsbad, CA, USA) according to manufacturers' recommendations. miRNA profiling was performed using 1 µg of total RNA according to the protocol described in the Supplementary Material.

Reverse-phase-protein array

126 specific antibodies (Supplementary Table 3) were analyzed on the 34 LCCL according to the protocol described in the Supplementary Material.

Single and combination drug screening

We analyzed 31 therapeutic compounds on the whole panel of 34 LCCL (Supplementary Table 4). Drug screening was performed using the HP D300 digital dispenser (Tecan) to create dose-response curves as described in the Supplementary Material.

Identification of biomarkers related to drug sensitivity

To identify molecular features associated with drug response we performed elastic net regression as described in the Supplementary Material.

Statistical analysis

Statistical analysis and data visualization were performed using both R software version 3.5.1 (R Foundation for Statistical Computing, Vienna, Austria. https://www.R-project.org) with Bioconductor packages and PRISM7 software (GraphPad Software, Inc., La Jolla, CA). Comparison of a continuous variable in 2 or more than 2 groups was performed using either parametric test (t-test or ANOVA) if the variable was normally distributed or non-parametric test (Mann-Whitney or Kruskal-Wallis test). Qualitative data were compared using the Fisher's exact test and Chi-squared test to compare binary and non-binary categorical variables, respectively. Correlation analysis between continuous variables was performed using Pearson r correlation when both variables were normally distributed with the assumptions of linearity and homoscedasticity or Spearman's rank-order correlation. All tests were two-tailed and P-value < 0.05 was considered as significant.

Tumors

The LICA-FR and TCGA cohorts of HCC patients including respectively 156 and 319 tumors cases were previously described.[15,16]

RESULTS

Liver cancer cell lines retain the genomic alterations identified in HCC tumors

We qualified and analyzed a total of 34 liver cancer cell lines (LCCL) including 32 derived from HCC and 2 from hepatoblastoma (HepG2 and Huh6) (Supplementary Table 1) that were compared to 821 HCC primary tumors including our HCC cohort (n=235),[17] and 2 independent public datasets from Korea (n=231),[18] and mixed Asian/European origin (n=355).[16] Male and female repartition was similar in LCCL and HCC tumors, while LCCL were enriched in HBV and HCV infections and patients were younger (median age 51 versus 60 years, $P<0.0001$) compared to HCC (Figure 1).

WES analysis identified a higher median mutation rate in LCCL compared to the 821 HCC primary tumors for both synonymous (median=81 versus 24) and non-synonymous mutations (median=339 versus 68) (Figure 1, Supplementary Figure 1A and Supplementary Table 5) that could be partly caused by the lack of available matched constitutional DNA resulting in undetectable germline rare variants. Mutational signature analysis taking into account the type of substitution and the trinucleotide context revealed that most of the mutations identified in LCCL were related to signature 1 and 5 both associated with age (Supplementary Figure 2). Signature 24, related to aflatoxin B1 exposure, was identified in PLC/PRF5 showing the highest number of mutations (n=949) from an African patient with a typical *TP53* R249 mutation (Supplementary Figure 2).

In LCCL, we identified mutations in 59 out of 72 cancer driver genes recurrently mutated in HCC from 5 publically available datasets (Figure 1, Supplementary Tables 2A-B and Supplementary Material). Mutational patterns of these genes were fairly similar in LCCL compared to HCC primary tumors (Spearman r=0.59 $P<0.0001$) (Figure 1). Also, 16 genes showed more frequent mutations in LCCL, including mutations in *TP53*, *AXIN1* and *FGF19*/*CCND1* amplification known to be associated with clinically aggressive HCC

classified in the "proliferation class".[19] In contrast, *CTNNB1* mutations belonging the "non-proliferation class" were less frequent in LCCL (15%) compared with primary tumors (29%). CNA analysis identified recurrent homozygous deletions of *CDKN2A*/*MTAP* and *AXIN1*, and focal amplification containing *CCND1* and *FGF19* in LCCL as in HCC (Supplementary Figure 1B). As previously described, in primary HCC major associations between risk factors and gene mutation were found between alcohol intake and *CTNNB1* and *TERT* promoter mutations and HBV infection and *TP53* mutations. In LCCL, we confirmed the significant association between HBV infection and *TP53* mutations (Supplementary Figure 3). In addition, 300 fusion transcripts were identified by RNA sequencing across the 34 LCCL. Among them, 51 involved cancer driver genes related to HCC (n=11) or to other cancer types (n=40) (Supplementary Table 6). We also detected 33 chimeric HBV-human fusion transcripts in 13 LCCL with recurrent insertions in *TERT* promoter (3/34), as previously reported in HCC primary tumors (Supplementary Table 7).[16,20] Overall, our panel of LCCL shared the most common genetic alterations identified in primary tumors recapitulating the genomic landscape of the most aggressive HCCs.

Transcriptomic identified 3 LCCL subgroups recapitulating the most aggressive subclasses of HCC

Unsupervised consensus classification of the RNA-sequencing data enabled to classify robustly 33/34 LCCL (except JHH1) defining 3 subgroups, CL1-3, further confirmed by principal component analysis (Figure 2A). CL1 included the most differentiated LCCL with epithelial features and an "hepatoblast-like" appearance, characterized by the expression of hepatocyte and liver fetal/progenitor markers (Figure 2B-C and Supplementary Tables 8-9). CL3 subgroup included less differentiated LCCL with more invasive, proliferative "mesenchymal-like" profile, expressing higher level of stem cell markers and EMT/metastasis

genes and low levels of hepato-specific genes (Figure 2B-C and Supplementary Table 8-9). CL2 subgroup displayed a mixed "epithelial-mesenchymal" pattern between CL1 and CL3 with an intermediate expression of hepato-specific genes and stem cell markers and a mild enrichment in *TSC2* and *NFE2L2* mutations (Figure 2B-C, Supplementary Table 8-9, Supplementary Figure 3). The distribution of the other HCC driver genes was not different between the 3 subgroups (Supplementary Figure 4). Using a centroid-based prediction method, we showed that LCCL transcriptomic subgroups were closely similar to the most aggressive HCC primary tumors subclasses previously established by Boyault (G1-G3) and Hoshida (S1-S2) corresponding to the "proliferation class" (Figure 2A).[21,22] CL1 was mainly similar to Boyault's-G1 and Hoshida's-S2 HCC subclasses whereas CL2 and CL3 subgroups corresponded to the Boyault's-G3 and Hoshida's-S1 subclasses (Figure 2A-B). However, the "non-proliferative", most differentiated and less aggressive HCC class (G4-G6 and S3) was not represented in our panel of LCCL. LCCL transcriptomic profiles showed remarkable stability compared with those from the external GDSC dataset (Supplementary Figure 5A).

miRNome and protein expression are closely associated with LCCL transcriptomic classification

We analyzed miRNA expression profiles by miRNA sequencing and the expression of 126 candidate proteins by RPPA in the 34 LCCL. Unsupervised classification of miRNA and protein expression profiles were strongly associated with the transcriptomic CL1-CL3 subgroups (Figure 3A-B). Five miRNA showed a significant differential expression between the 3 LCCL transcriptomic subgroups including miR-1257 and two members of the miR-122, and miR-194 family (Figure 3A and Supplementary Table 10). Except for miR-1257 showing the highest expression in CL1 and the lowest expression in CL2 subgroup, expression of miR-122-5p, miR-122-3p, miR-194-5p and miR-194-3p was closely related to the degree of LCCL

differentiation with the highest and lowest level in CL1 and CL3 subgroups, respectively (Figure 3A and Supplementary Table 10). Accordingly, miR-122-5p was reported as liver-specific and represents the most abundant miRNA in mature hepatocytes.[23] In the same line, miR-194-5p was described as a liver epithelial cell marker and its downregulation increased EMT and HCC metastasis in preclinical models.[24]

The 126 proteins analyzed by RPPA included 82 total proteins and 44 phospho-proteins involved in various signaling pathways (Supplementary Table 3 and Supplementary Table 11). Messenger RNA and their corresponding protein expressions were closely related together (Spearman's r=0.25 versus random protein/mRNA pairs r=0.002; $P<0.0001$, Mann-Whitney test), comparable to previous studies on tumor samples (mean Spearman's r=0.3[25]) (Supplementary Figure 6 and Supplementary Table 12). We identified 19 proteins significantly differentially expressed between LCCL transcriptomic subgroups (Figure 3B and Supplementary Figure 7). Protein expression profiles reflected the differentiation state of LCCL with proteins expressed in mature hepatocytes (ALDH1A1, E-cadherin, p190A, RSK2, HER3, FGFR4) that were dramatically downregulated in CL3 subgroup and expression of the hepatic progenitor marker cytokeratin 19 that was higher in CL1 and CL2 subgroups (Figure 3B). Protein expression identified a more pronounced activation of the TGFß (TGFß-I-III and phospho-SMAD2/3) and the non-canonical ß-catenin pathways (phosphoSer675) in CL2 and CL3 subgroups (Figure 3B).

We also identified two major networks of protein co-regulation in the whole panel of LCCL with proteins involved in DNA repair, cell cycle, apoptosis and in the PI3K/AKT/mTOR pathway (Figure 3C). Finally, investigating relationship between protein expression and the mutational status of the HCC driver genes mutated in LCCL yielded 268 significant associations (Supplementary Table 13). As expected, cyclin D1 was overexpressed in LCCL harboring co-amplification of *CCND1* and *FGF19*. AXIN1 protein was overexpressed in the

CTNNB1 mutated LCCL. In addition, consistent with their inactivation, mutations in the tumor suppressor genes (TSG) *TSC2* and *AXIN1* were associated with the downregulation of the corresponding proteins, we also found a known association between inactivating mutations of *KEAP1* and overexpression of NQO1 protein (Figure 4D).

Drug screening and molecular features associated with drug sensitivity

In our panel of 34 LCCL we screened 31 drugs including compounds approved or in clinical development in HCC or other cancers and targeting key pathways of liver tumorigenesis (Figure 4A and Supplementary Table 4 and 14). We also analyzed four drug combinations with sorafenib including the AKT inhibitor MK-2206, the HDAC inhibitor resminostat and the two MEK1/2 inhibitors trametinib and refametinib.

We showed that the most potent drugs were those that target general processes, such as proteasome, mitosis or protein folding (Figure 4A). Of note inhibitors targeting both PI3K/mTOR or mTOR alone were among the 7 most effective drugs with a median AUC close to doxorubicin, a chemotherapeutic agent used to treat HCC by transarterial chemoembolization (Figure 4A). Surprisingly, sorafenib, lenvatinib, cabozantinib and regorafenib that are multikinase inhibitors used in first or second line systemic treatment of HCC, showed mild efficiency and were ranked at the 26^{th}, 25^{th}, 31^{th} and 34^{th} position, respectively (Figure 4A). Remarkably, the MEK1/2 inhibitor trametinib showed the highest variable responses within the 34 LCCL. The combination of sorafenib either with the AKT inhibitor MK-2206 or the anti-HDAC resminostat produced an additive effect in inhibiting cell viability, as indicated by a median combination index (CI) of 1.1 and 1.2, respectively (Figure 4D and Supplementary Table 14). Strikingly, sorafenib showed synergistic effect when combined with MEK1/2 inhibitors in around 60-70% of the cell lines (Figure 4D), that was more pronouced with trametinib (Figure 4A). Overall, there was a good correlation between AUC and GI50 values (Supplementary Figure 8) and, our drug sensitivity profiles

were well correlated with those from the external GDSC LCCL dataset (Supplementary Figure 5B).

Unsupervised hierarchical clustering of drug responses on the whole series of 34 LCCL showed common sensitivity profiles for drugs with similar mechanism of action and identified two main subgroups of LCCL associated with transcriptomic subgroups (P<0.009) (Figure 4B). Accordingly, the global drug response rate was higher in the most differentiated CL1 subgroup, compared with CL2 and CL3 subgroups that were less differentiated and resistant to most of the analyzed compounds (Figure 4C). Of note, cabozantinib, targeting multiple kinases including c-MET showed a pharmacological profile close to the two selective MET inhibitors (PHA-665752 Spearman's r=0.38, P=0.02 and JNJ-38877605 Spearman's r=0.39, P=0.02) (Figure 4B).

We identified 8 drugs and 3 combinations showing different sensitivity pattern according to the transcriptomic subgroups (Figure 4D). Among them, 6 drugs including cabozantinib (multi-kinase inhibitor), linsitinib (anti-IGF1R), alvespimycin (anti-HSP90), JNJ-38877605 (anti-MET), nutlin 3 (anti-MDM2) and the combination sorafenib-MK2206, showed a higher sensitivity specifically in the CL1 subgroup. Of note, for the combination sorafenib-MK2206 (anti-AKT) the median CI was 0.9 in CL1 compared to 1.2 for CL2 and CL3 subgroups indicating a synergistic effect of the combination in at least half of the CL1 cell lines (Supplementary Table 14). Refametinib (anti-MEK) and tanespimycin (anti-HSP90) were more efficient in CL1 compared with CL3 subgroup, while trametinib (anti-MEK1/2) showed higher efficiency both in CL1 and CL2 subgroups. Combination of sorafenib either with trametinib or refametinib was more potent both in CL1 and CL2 subgroups. We also identified 312 drug-protein predictive pairs (Figure 4E and Supplementary Table 15). Among them, we validated the association between the high expression level of NQO1 and the high sensitivity to the two HSP90 inhibitors, alvespimycin and tanespimycin.[9,10,26] Expression of

cytokeratin 19 was strongly associated with higher sensitivity to dasatinib (src-inhibitor), in agreement with the higher dasatinib vulnerability in a "progenitor-like" subtype of LCCL.[27] In our study, cytokeratin 19 expression was also associated with higher response to trametinib (anti-MEK1/2) and navitoclax (anti Bcl-2, Bcl-XL, and Bcl-w).

We also identified 143 significant associations between genetic alterations and drug sensitivity (Supplementary Tables 16 and 17) among which, *TSC1*/*TSC2* inactivating mutations were linked with a higher sensitivity to the mTOR inhibitor rapamycin (Figure 4F). In addition, we confirmed in our large panel of LCCL, the hypersensitivity to the AURKA inhibitor Alisertib in the *TP53*-mutated cell lines (Figure 4F).[28] Interestingly, the only *MET*-amplified cell line (MHCC97H, Figure 4D) was highly sensitivity to the two selective MET inhibitors (PHA-665752 and JNJ-38877605) as well as cabozantinib (Figure 4D and Supplementary Table 14).

In order to explore among all the molecular features (genomic alterations, miRNA and mRNA expression), those that were the most associated with drug response, we used elastic net (EN) regression. This analysis yielded a huge number of molecular markers linked to drug response with a median of 95 associated features per drug (min: 0, max: 139), when using an EN score $\geq$0.7 (Supplementary Figure 9 and Supplementary Table 18-19) and uncovered strong associations in particular, between sensitivity to the MEK1/2 inhibitors trametinib and refametinib and expression of *HSD17B7* (see next paragraph). We could not identify strong predictors for lenvatinib and regorafenib because of their poor *in vitro* efficiency. However, elastic net analysis identified high mRNA level of *PRMT5* and *GPS1* as the best predictors of sorafenib sensitivity and *STEAP2* and *STEAP1* expression as strong predictors of cabozantinib sensitivity. In contrast, resistance to the two drugs was predicted by overexpression of *UBE2H* and *SLC25A29* for sorafenib and *NBAS* and *LAPTMA4* for cabozantinib (Supplementary Table 19). Among the different features analyzed, mRNA

expression showed the best predictive value, while miRNA expression and genomic alterations were poorly predictive of drug response, even when adjusting on the number of tested features (Supplementary Figure 9 and Supplementary Table 18).

Sensitivity to the MEK inhibitor trametinib is related to RAS-MAPK genomic alterations and cell differentiation

We focused our analysis on the MEK inhibitor trametinib, that showed a bimodal sensitivity pattern, with a group of highly sensitive and a group of resistant LCCL (Figure 5A). We identified oncogenic alterations known to activate the RAS-MAPK pathway in half of the LCCL (Figure 5A). All these genomic alterations were mutually exclusive, they affected 4 oncogenes (*FGF19* and *MET* amplifications, *NRAS* Q61L mutation and *ERBB4* fusion), and 2 TSG (*RPS6KA3* and *NF1*) (Figure 5A-B and Supplementary Figure 10). We identified an enrichment of the RAS-MAPK pathway genomic alterations in the most sensitive LCCL to trametinib (10/14; 71%) compared to those that were resistant (7/20; 35%) while it did not reach statistical significance (P=0.08, Fisher's exact test) (Figure 5A). Intriguingly, among the 11 *FGF19*-amplified cell lines, nearly half of them (5/11) were not sensitive to trametinib and they showed highly variable levels of *FGF19* mRNA not explained by *FGF19* copy number (Figure 5A and Supplementary Figure 10A). Strikingly, expression of *FGF19* in LCCL was both dependent on gene amplification and on the transcriptomic subgroup with the highest expression in the most differentiated CL1 subgroup and the lowest expression in the poorly differentiated CL3 subgroup both in amplified and non-amplified LCCL (Figure 5A). In contrast, *CCND1* that was invariably co-amplified with *FGF19*, was overexpressed in all the amplified LCCL whatever the transcriptomic subgroup (Supplementary Figure 10A). Moreover, the 3 other key components of the FGF19/FGFR4 pathway including FXR (encoded by *NR1H4*) known to transactivate *FGF19* were co-

regulated together with *FGF19* in LCCL (Figure 5C). Accordingly, within the *FGF19*-amplified cell lines, we identified a strong correlation between trametinib sensitivity and *FGF19* mRNA level (Figure 5D). A similar association was observed with the two FGFR4 inhibitors BLU-9931 and H3B-6527, which reinforce the link between trametinib sensitivity, *FGF19* amplification and expression (Figure 5D). Altogether, these results revealed that *FGF19* amplification solely is not sufficient to predict sensitivity to both trametinib and FGFR4 inhibitors but the expression of a full pathway modulated by the context of differentiation is required.

Then, we searched for robust predictors of trametinib response among all the molecular features analyzed using elastic net regression. We identified 5 genes (*HSD17B7, RORC, MRPS14, SERINC2, LAD1)* with a high mRNA expression associated with higher trametinib sensitivity, named "trametinib 5 gene-score" to predict accurately the response (Figure 5E and Supplementary Table 19). We validated these results in the GDSC external dataset (Supplementary Figure 11). In primary HCC, both in TCGA (n=319) and LICA-FR (n=156) datasets, the G3 and S1 transcriptomic subclasses expressed the lowest level of the signature (Figure 6A and Supplementary Figure 12). In tumors, we also showed that the mean expression of the FGF19/FGFR4 pathway varied according to the transcriptomic subclasses of HCC in the two datasets with the highest expression in the G1 and S2 subclasses and the lowest expression in the G3 and S1 subclasses. Interestingly, expression of the "trametinib 5 gene-score" signature was highly correlated with the mean expression of the FGF19/FGFR4 pathway in both datasets (Spearman's r=0.4, $P<0.0001$ for TCGA cohort, Spearman's r=0.33, $P<0.0001$ for LICA-FR cohort) (Figure 6A and Supplementary Figure 12).

In HCC primary tumors, 24 focal amplifications of the 11q13.3 region were identified in the TCGA series, including 21 cases with both *FGF19* and *CCND1* amplification and 3 cases with *CCND1* amplification alone (Figure 6B). As observed in LCCL, *FGF19* mRNA

expression in tumors was related to both the gene amplification and the transcriptomic subclass, with no *FGF19* overexpression when amplifications occurred in the G3 and S1 subclasses, showing lower expression of *NR1H4* (Figure 6A-B). By contrast, as in cell lines, *CCND1* was invariably overexpressed in the amplified tumors whatever the transcriptomic subclass suggesting that only FGF19 expression was sensitive to the differentiation context. Overall, G1/S2 subclasses of HCC may be the best candidate for a trametinib or anti-FGFR4 therapy while G3/S1 subclasses are unlikely to respond.

DISCUSSION

In the present study, we showed that our panel of LCCL recapitulates the diversity of the most aggressive "proliferation class" of HCC both at the genomic and transcriptomic levels and this is a unique tool to translate our understanding of liver cancer development into therapeutics (summarized in Figure 7).

By combining genomic, transcriptomic and protein profile analysis in our panel of 34 LCCL, we identified strong similarities with the established HCC molecular subclasses, suggesting that LCCL are representative models of primary tumors. We identified three robust transcriptomic subgroups of LCCL driven by the differentiation state and sharing features similar to those described in HCC tumors. The CL1 "hepatoblast-like" subgroup of cell lines expresses hepato-specific genes and fetal/progenitor markers, it corresponds to the "progenitor subclass" of HCC.[19] CL2 "mixed epithelial-mesenchymal" and CL3 "mesenchymal-like" subgroups were less differentiated with an activation of the TGFß and non-canonical ß-catenin pathways, they were more similar to the "Wnt-TGFß"[22] and Boyault's G3 subclasses of HCC[21] (Figure 7). The high expression of EMT-metastasis genes is another feature of the CL2 and CL3 subgroups of LCCL that may result from the aberrant activation of the TGFß pathway.[29] However, consistent with the underrepresentation of *CTNNB1* mutations in LCCL, the less aggressive "non-proliferation class" of HCC was not represented in our panel of LCCL and of note even those cell lines mutated for *CTNNB1* did not properly reflect the *CTNNB1* mutated subclass of primary HCC as they were all classified in the proliferation class and showed *TP53* mutations, representing only a small and atypical fraction of primary HCC mutated for *CTNNB1* (Supplementary Figure 13). These observations may be explained by the selection of the most aggressive phenotypes during cell line establishment that favors cells with the best survival capabilities. Additional LCCL are needed to represent the "non-proliferation class", which should be feasible with the

development of new cell culture techniques such as those using Rho-kinases inhibitors.

Our findings provided novel insights regarding the crucial interplay between the differentiation context, the genetic alterations and drug response in HCC (summarized in Figure 7). Strikingly, the global drug response rate among LCCL was related to the transcriptomic subgroup and the cell differentiation state with the most differentiated CL1 subgroup showing the highest drug sensitivity.

Cell differentiation also interferes with specific signaling pathways. *FGF19* amplification is a very appealing therapeutic target with the development of selective inhibitors of its receptor, FGFR4.[30,31] However, *FGF19* amplifications were not always associated with its overexpression both in LCCL and HCC tumors. We showed that only LCCL expressing a hepatocyte differentiation program with conserved expression of the FXR transcription factor and of the receptor complex, including FGFR4 and KLB, were sensitive to the FGFR4 inhibitors, which extends other previous findings.[30–32] Remarkably, this group of LCCL was also highly sensitive to inhibition of MEK1/2, an effector downstream FGF19/FGFR4, with trametinib, which is already approved in *BRAF*-mutated melanoma.[33] In LCCL, trametinib has demonstrated higher potency than the anti-FGFR4 BLU-9931 thereby representing a new attractive drug for targeting HCC addicted to the FGF19/FGFR4 pathway. Accumulating evidence indicate that the differentiation context plays a determinant role in treatment response, in particular it was shown that a therapy targeting a specific mutation will not necessarily have the same efficacy in tumors sharing the same mutation but arising in different tissue types.[34] In this line, a recent report demonstrated that gene expression and the tissue of origin predicted much better drug sensitivity in pan-cancer cell line analysis than genetic alterations.[35] Here, we showed that this concept could be also generalized to tumors from the same organ. Interestingly, trametinib is also efficient in LCCL harboring other alterations in the RAS-MAPK pathway such as *RPS6KA3* inactivation or *MET* amplification.

However, *MET* amplifications, even if they are rare events, are more efficiently targeted by specific MET inhibitors including cabozantinib and these findings could be translated in the clinics as we confirmed recently MET oncogenic addiction in a patient with an advanced HCC amplified for MET, who achieved a complete tumor response after treatment by teponinib, a specific Met inhibitor.[36] Our study has also highlighted a synergistic effect of sorafenib in combination with MEK1/2 inhibitors with higher sensitivity in the CL1 and CL2 subgroups of LCCL, in lines with recent studies in HCC preclinical models and in HCC patients.[37,38]

Our screening also identified potential new attractive drugs already approved in the clinics in specific molecular contexts. Our results showed responses in LCCL harboring inactivating mutations in *TSC1* or *TSC2* treated by an mTOR inhibitor, suggesting that the 7% of HCC demonstrating the same alterations could benefit from rapamycin or alternative inhibitors, in line with previous reports (Figure 7).[16,18,39–41] Dasatinib also showed enhanced efficiency in LCCL expressing high levels of cytokeratin 19.[27] We recently reported a specific enrichment of immunohistochemical expression of CK19 in the "progenitor subclass" of HCC which may represent a good candidate for dasatinib therapy.[41] Additionally, we identified other potential drugs that may specifically target the "progenitor subclass" of HCC such as linsitinib, an inhibitor of IGF1R, or sorafenib in combination with the anti-AKT MK-2204. Indeed, linsitinib hypersensitivity in the CL1 subgroup of LCCL, that recapitulates the "progenitor subclass" of HCC, is consistent with the strong overexpression of IGF2. Accordingly, a recent work in transgenic mice demonstrated the pro-oncogenic role of IGF2 in the liver and showed that blocking IGF2 by an antibody efficiently impaired growth of liver tumor cells overexpressing IGF2, *in vitro* and *in vivo*.[42] In the present work, we also enlighten the specific vulnerability of *TP53*-mutated LCCL to the AURKA inhibitor alisertib corroborating a recent study in mice.[28] Thus, alisertib may represent a new therapeutic opportunity for P53 mutated

HCC patients, as *TP53* is the most frequently mutated TSG in HCC and, until now, was considered to be undruggable. The lack of biomarker-driven clinical trials may partly explain why some drugs that appear to be effective *in vitro* such as rapamycin, tivantinib or dasatinib failed in patients. Unexpectedly, gold standard therapies for advanced HCC including sorafenib, lenvatinib, cabozantinib and regorafenib showed poor efficiency in LCCL suggesting that they have only limited anti-proliferative effect on liver tumor cells but more likely target tumor microenvironment. Accordingly, all the effective drugs in HCC share an anti-angiogenic activity that could not be explored *in vitro* and represents a limitation in the use of cellular models.

In conclusion, our work showed that LCCL represent a valuable and powerful resource for drug-biomarker discovery that may be useful to guide future clinical trials. Moreover, this study provides a comprehensive molecular characterization of the most widely used LCCL that are freely accessible on our website: http://lccl.zucmanlab.com

REFERENCES

1. Llovet JM, Ricci S, Mazzaferro V, et al. Sorafenib in advanced hepatocellular carcinoma. N Engl J Med 2008;359:378–390.

2. Kudo M, Finn RS, Qin S, et al. Lenvatinib versus sorafenib in first-line treatment of patients with unresectable hepatocellular carcinoma: a randomised phase 3 non-inferiority trial. Lancet 2018;391:1163–1173.

3. Bruix J, Qin S, Merle P, et al. Regorafenib for patients with hepatocellular carcinoma who progressed on sorafenib treatment (RESORCE): a randomised, double-blind, placebo-controlled, phase 3 trial. Lancet 2017;389:56–66.

4. Zhu AX, Kang Y-K, Yen C-J, et al. Ramucirumab after sorafenib in patients with advanced hepatocellular carcinoma and increased α-fetoprotein concentrations (REACH-2): a randomised, double-blind, placebo-controlled, phase 3 trial. Lancet Oncol 2019.

5. Abou-Alfa GK, Meyer T, Cheng A-L, et al. Cabozantinib in Patients with Advanced and Progressing Hepatocellular Carcinoma. N Engl J Med 2018;379:54–63.

6. El-Khoueiry AB, Sangro B, Yau T, et al. Nivolumab in patients with advanced hepatocellular carcinoma (CheckMate 040): an open-label, non-comparative, phase 1/2 dose escalation and expansion trial. Lancet 2017;389:2492–2502.

7. Bruix J, Reig M, Rimola J, et al. Clinical decision making and research in hepatocellular carcinoma: pivotal role of imaging techniques. Hepatology 2011;54:2238–2244.

8. Shoemaker RH. The NCI60 human tumour cell line anticancer drug screen. Nat Rev Cancer 2006;6:813–823.

9. **Barretina J, Caponigro G, Stransky N**, et al. The Cancer Cell Line Encyclopedia enables predictive modelling of anticancer drug sensitivity. Nature 2012;483:603–607.

10. **Garnett MJ, Edelman EJ, Heidorn SJ**, et al. Systematic identification of genomic

markers of drug sensitivity in cancer cells. Nature 2012;483:570–575.

11. Rebouissou S, Zucman-Rossi J, Moreau R, et al. Note of caution: Contaminations of hepatocellular cell lines. J Hepatol 2017;67:896–897.

12. Nault JC, Mallet M, Pilati C, et al. High frequency of telomerase reverse-transcriptase promoter somatic mutations in hepatocellular carcinoma and preneoplastic lesions. Nat Commun 2013;4:2218.

13. Shinde J, Bayard Q, Imbeaud S, et al. Palimpsest: an R package for studying mutational and structural variant signatures along clonal evolution in cancer. Bioinformatics 2018;34:3380–3381.

14. Ritchie ME, Phipson B, Wu D, et al. limma powers differential expression analyses for RNA-sequencing and microarray studies. Nucleic Acids Res 2015;43:e47.

15. Bayard Q, Meunier L, Peneau C, et al. Cyclin A2/E1 activation defines a hepatocellular carcinoma subclass with a rearrangement signature of replication stress. Nat Commun 2018;9:5235.

16. Cancer Genome Atlas Research Network. Electronic address: wheeler@bcm.edu, Cancer Genome Atlas Research Network. Comprehensive and Integrative Genomic Characterization of Hepatocellular Carcinoma. Cell 2017;169:1327-1341.e23.

17. **Schulze K, Imbeaud S, Letouzé E**, et al. Exome sequencing of hepatocellular carcinomas identifies new mutational signatures and potential therapeutic targets. Nat Genet 2015;47:505–511.

18. Ahn S-M, Jang SJ, Shim JH, et al. Genomic portrait of resectable hepatocellular carcinomas: implications of RB1 and FGF19 aberrations for patient stratification. Hepatology 2014;60:1972–1982.

19. Llovet JM, Montal R, Sia D, et al. Molecular therapies and precision medicine for hepatocellular carcinoma. Nat Rev Clin Oncol 2018;15:599–616.

20. **Zhao L-H, Liu X, Yan H-X,** et al. Genomic and oncogenic preference of HBV integration in hepatocellular carcinoma. Nat Commun 2016;7:12992.

21. Boyault S, Rickman DS, Reyniès A de, et al. Transcriptome classification of HCC is related to gene alterations and to new therapeutic targets. Hepatology 2007;45:42–52.

22. Hoshida Y, Nijman SMB, Kobayashi M, et al. Integrative transcriptome analysis reveals common molecular subclasses of human hepatocellular carcinoma. Cancer Res 2009;69:7385–7392.

23. Deng X-G, Qiu R-L, Wu Y-H, et al. Overexpression of miR-122 promotes the hepatic differentiation and maturation of mouse ESCs through a miR-122/FoxA1/HNF4a-positive feedback loop. Liver Int 2014;34:281–295.

24. Meng Z, Fu X, Chen X, et al. miR-194 is a marker of hepatic epithelial cells and suppresses metastasis of liver cancer cells in mice. Hepatology 2010;52:2148–2157.

25. **Akbani R, Ng PKS, Werner HMJ**, et al. A pan-cancer proteomic perspective on The Cancer Genome Atlas. Nat Commun 2014;5:3887.

26. Kelland LR, Sharp SY, Rogers PM, et al. DT-Diaphorase expression and tumor cell sensitivity to 17-allylamino, 17-demethoxygeldanamycin, an inhibitor of heat shock protein 90. J Natl Cancer Inst 1999;91:1940–1949.

27. Finn RS, Aleshin A, Dering J, et al. Molecular subtype and response to dasatinib, an Src/Abl small molecule kinase inhibitor, in hepatocellular carcinoma cell lines in vitro. Hepatology 2013;57:1838–1846.

28. Dauch D, Rudalska R, Cossa G, et al. A MYC-aurora kinase A protein complex represents an actionable drug target in p53-altered liver cancer. Nat Med 2016;22:744–753.

29. Zavadil J, Böttinger EP. TGF-beta and epithelial-to-mesenchymal transitions. Oncogene 2005;24:5764–5774.

30. Joshi JJ, Coffey H, Corcoran E, et al. H3B-6527 Is a Potent and Selective Inhibitor of

FGFR4 in FGF19-Driven Hepatocellular Carcinoma. Cancer Res 2017;77:6999–7013.

31. Hagel M, Miduturu C, Sheets M, et al. First Selective Small Molecule Inhibitor of FGFR4 for the Treatment of Hepatocellular Carcinomas with an Activated FGFR4 Signaling Pathway. Cancer Discov 2015;5:424–437.

32. Gao Q, Wang Z-C, Duan M, et al. Cell Culture System for Analysis of Genetic Heterogeneity Within Hepatocellular Carcinomas and Response to Pharmacologic Agents. Gastroenterology 2017;152:232-242.e4.

33. **Flaherty KT, Robert C**, Hersey P, et al. Improved survival with MEK inhibition in BRAF-mutated melanoma. N Engl J Med 2012;367:107–114.

34. **Prahallad A, Sun C, Huang S**, et al. Unresponsiveness of colon cancer to BRAF(V600E) inhibition through feedback activation of EGFR. Nature 2012;483:100–103.

35. Iorio F, Knijnenburg TA, Vis DJ, et al. A Landscape of Pharmacogenomic Interactions in Cancer. Cell 2016;166:740–754.

36. Nault JC, Martin Y, Caruso S, et al. Clinical impact of genomic diversity from early to advanced hepatocellular carcinoma. Hepatology 2019:In Press.

37. Wang C, Jin H, Gao D, et al. Phospho-ERK is a biomarker of response to a synthetic lethal drug combination of sorafenib and MEK inhibition in liver cancer. J Hepatol 2018;69:1057–1065.

38. Lim HY, Merle P, Weiss KH, et al. Phase II Studies with Refametinib or Refametinib plus Sorafenib in Patients with RAS-Mutated Hepatocellular Carcinoma. Clin Cancer Res 2018;24:4650–4661.

39. Schulze K, Imbeaud S, Letouzé E, et al. Exome sequencing of hepatocellular carcinomas identifies new mutational signatures and potential therapeutic targets. Nat Genet 2015;47:505–511.

40. **Ho DWH, Chan LK**, Chiu YT, et al. TSC1/2 mutations define a molecular subset of

HCC with aggressive behaviour and treatment implication. Gut 2017;66:1496–1506.

41. Calderaro J, Couchy G, Imbeaud S, et al. Histological subtypes of hepatocellular carcinoma are related to gene mutations and molecular tumour classification. J Hepatol 2017;67:727–738.

42. Martinez-Quetglas I, Pinyol R, Dauch D, et al. IGF2 Is Up-regulated by Epigenetic Mechanisms in Hepatocellular Carcinomas and Is an Actionable Oncogene Product in Experimental Models. Gastroenterology 2016;151:1192–1205.

Author names in bold designate shared co-first authorship

FIGURES LEGENDS

Figure 1. Mutational landscape of driver genes in 34 LCCL compared with HCC primary tumors. Top panel shows total (putative somatic) mutation rate for each cell line. The heatmap represents mutations and CNA of the 59 HCC-associated genes mutated in LCCL. On the left, histograms showing comparison of gene alteration frequency between LCCL and HCC (Fisher's exact test, *P*-value: * <0.05; ** <0.001; *** <0.0001 and Spearman's correlation). In the bottom, pie charts and histograms comparing the distribution of viral infection, gender (Fisher's exact test) and age (Mann-Whitney test) between HCC and LCCL.

Figure 2. Transcriptomic analysis of 34 LCCL. A) Consensus clustering and principal component analysis (PCA) of LCCL mRNA expression profiles for the optimal number of clusters at k=3 and association with Hoshida's and Boyault's HCC transcriptomic subclasses (Chi-square test). **B)** Gene set enrichment analysis (GSEA) showing the four main categories of gene sets enriched in each group of LCCL (FDR<0.01; normalized enrichment score (ES)>4 (red bars) in at least one LCCL group) (see also Supplementary Table 8). **C)** Expression pattern of genes related to liver differentiation, EMT-metastasis and proliferation differentially expressed between the 3 subgroups of LCCL (ANOVA test) (see also Supplementary Table 9). Horizontal line represents the median.

Figure 3. miRNA and protein profiles analysis in 34 LCCL. A) Left panel, consensus clustering of LCCL miRNA expression profiles (at k=3) and association with transcriptomic subgroups (Chi-square test). Right panel, number of miRNA differentially expressed between each transcriptomic subgroup of LCCL, median expression (horizontal line) per subgroup is shown for the 5 differentially expressed miRNAs between the 3 LCCL subgroups and

expression per LCCL is represented on the heatmap (see also Supplementary Table 10). **B)** Left panel, hierarchical clustering of LCCL protein profiles and association with transcriptomic subgroups (Chi-square test). Right panel, boxplots of the 19 proteins differentially expressed between LCCL transcriptomic subgroups (Mann-Whitney test) (see also Supplementary Table 11 and Supplementary Figure 5). **C)** Protein interaction network showing the most significant positive (red lines) and negative (blue dashed lines) correlations between protein pairs across LCCL. **D)** Volcano plot comparing protein expression according to the mutational status of HCC driver genes. Blue and red points represent protein-gene mutation interaction, and indicate proteins underexpressed and overexpressed in LCCL when the gene (in italics) is mutated, respectively. Only interactions with a *P*-value <0.01 and a Log_2 ratio>1 are shown (see also Supplementary Table 13).

Figure 4. Drug responses and associated molecular features in 34 LCCL. A) Top panel, pathways and biological processes targeted by the panel of tested drugs. Below, boxplots showing for each drug the distribution of sensitivity values across LCCL. + indicates the mean. Bold: drugs approved in HCC. **B)** Hierarchical clustering showing patterns of sensitivity to 31 drugs and 4 combinations in LCCL and association with transcriptomic subgroups (Chi-square test). AUC values in rows were centered and scaled (z-score). At the bottom, boxplots comparing Spearman's rank correlation coefficients (left) and *P*-values (right) between AUC of drug pairs with identical or different molecular targets. **C)** Violin plots representing the distribution of AUC values for the whole panel of drugs according to LCCL transcriptomic subgroup. Tin black line: SD; black dot: median. **D)** Left panel, boxplots for the 11 drugs/combinations with different sensitivity profiles between LCCL transcriptomic subgroups (Red dot: MHCC97H, *MET*-amplified cell line). Right panel, the Combination Index distribution is shown for the four drug combinations (see also

Supplementary Table 14). **E)** Volcano plot of Spearman's correlations and significance between drug sensitivity (AUC) and protein expression. Blue and Red dots indicate respectively the most significant negative and positive correlations (*P*-value<0.05, and Spearman's r>0.5) (see also Supplementary Table 15). **F)** Sensitivity to rapamycin and alisertib and mutational status of *TSC1/TSC2* and *TP53* genes (see also Supplementary Table 16).

Statistical difference between groups was determined by a Mann-Whitney test in panels B, C, D and F.

Figure 5. Alteration of the RAS-MAPK pathway and trametinib sensitivity in 34 LCCL. **A)** Trametinib sensitivity, genomic alterations of the RAS-MAPK and their consequence on mRNA and protein expression in LCCL (see also Supplementary Figure 6). Difference in *FGF19* mRNA according to the gene amplification status and the transcriptomic subgroups was assessed by a two-way ANOVA. **B)** Schematic representation of oncogenic alterations of the RAS-MAPK pathway identified in LCCL and drugs analyzed in the present study (H3B-6527 was evaluated in another study[30]). **C)** mRNA expression of the key components of the FGF19/FGFR4 pathway, difference between groups was assessed using an ANOVA test and correlations between each component of the pathway by a Pearson's test. **D)** Correlation between sensitivity of drugs targeting MEK1/2 or FGFR4 and *FGF19* mRNA expression in *FGF19* amplified LCCL (Spearman's test). **E)** Volcano plot and heatmap showing the 10-top mRNA predictive of trametinib response identified by EN regression (see also Supplementary Table 19). On the right below, correlation between trametinib response and the mean expression of the 5 mRNA (green) overexpressed in sensitive LCCL ("trametinib 5-gene score") (Spearman's test).

Variance stabilized values were used for mRNA level except for *MET* and *ERBB4*.

Figure 6. Transcriptional expression of the "trametinib 5-gene score" and the key components of the FGF19/FGFR4 pathway in HCC according to the transcriptomic classifications. **A)** Boxplots showing expression of the "trametinib 5-gene score" and the mean mRNA level of the FGF19/FGFR4 pathway according to Boyault's and Hoshida's transcriptomic classifications; below, mean expression level +/- SD is shown for each component of the FGF19/FGFR4 pathway. The color scale below each boxplot indicates mRNA level per sample (Red: high expression, Blue: low expression), ranked in each transcriptomic subclass by the "trametinib 5-gene score". Differences between transcriptomic subclasses were assessed using ANOVA. Variance stabilized values were used for mRNA level. **B)** On the top: schematic representation of the 11q13.3 genomic region containing *CCND1* and *FGF19*. At the bottom, Tukey boxplots showing mRNA expression of *CCND1* and *FGF19* according to their amplification status and HCC transcriptomic subclass.

Figure 7. Summary of HCC molecular classes previously established and their corresponding LCCL subgroups with the main drug/biomarker pairs associations identified in the present study. HCC molecular classes and associated features were extracted from previous reports.[19,41] Ampl: amplification; mut: mutation

Figure 1

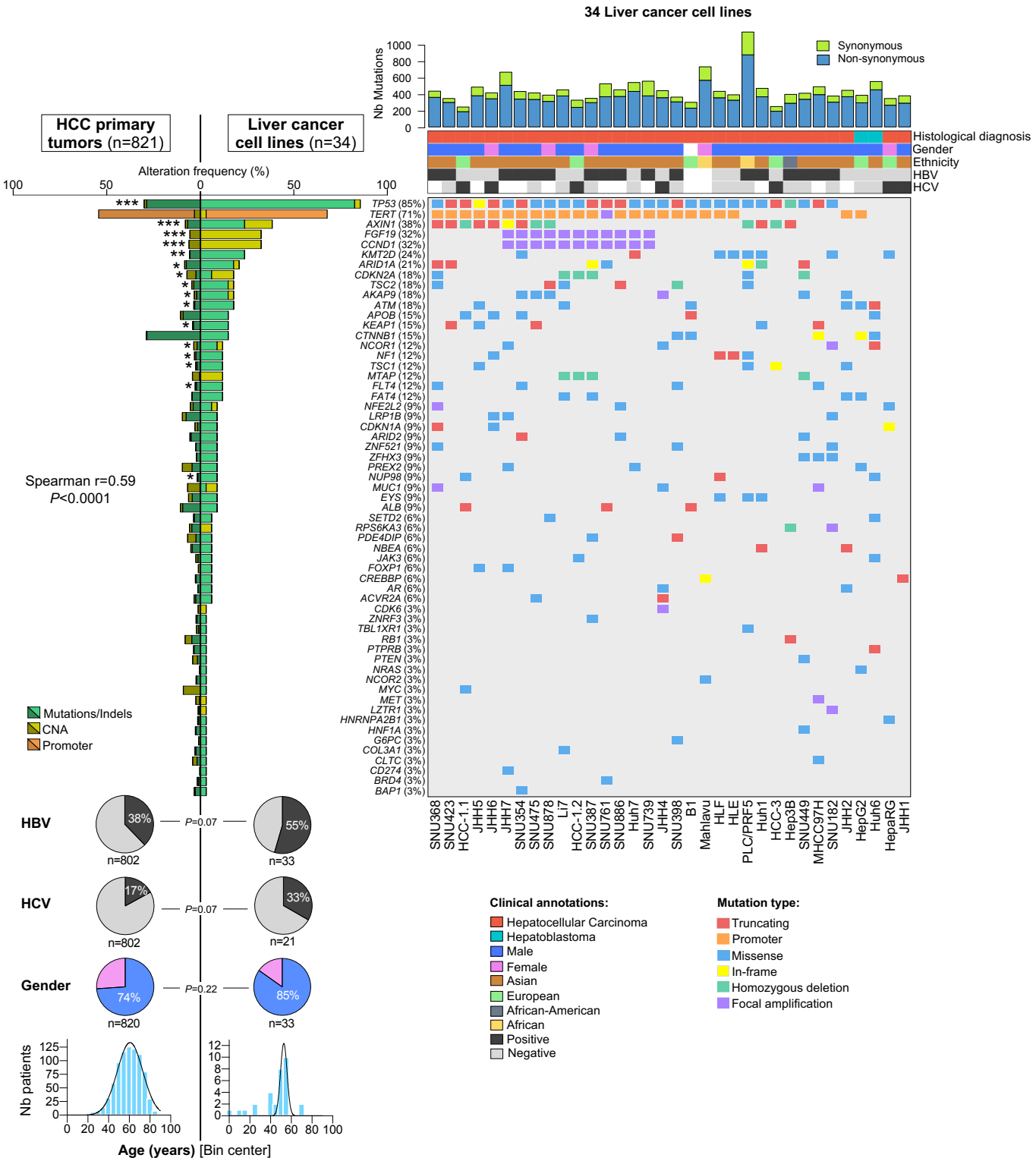
34 Liver cancer cell lines
Nb Mutations
Synonymous
Non-synonymous
Histological diagnosis
Gender
Ethnicity
HBV
HCV
HCC primary tumors (n=821)
Liver cancer cell lines (n=34)
Alteration frequency (%)
Spearman r=0.59
P<0.0001
Mutations/Indels
CNA
Promoter
HBV
HCV
Gender
P=0.07
P=0.07
P=0.22
38%
55%
17%
33%
74%
85%
n=802
n=33
n=802
n=21
n=820
n=33
Nb patients
Age (years) [Bin center]
Clinical annotations:
Hepatocellular Carcinoma
Hepatoblastoma
Male
Female
Asian
European
African-American
African
Positive
Negative
Mutation type:
Truncating
Promoter
Missense
In-frame
Homozygous deletion
Focal amplification

Figure 2

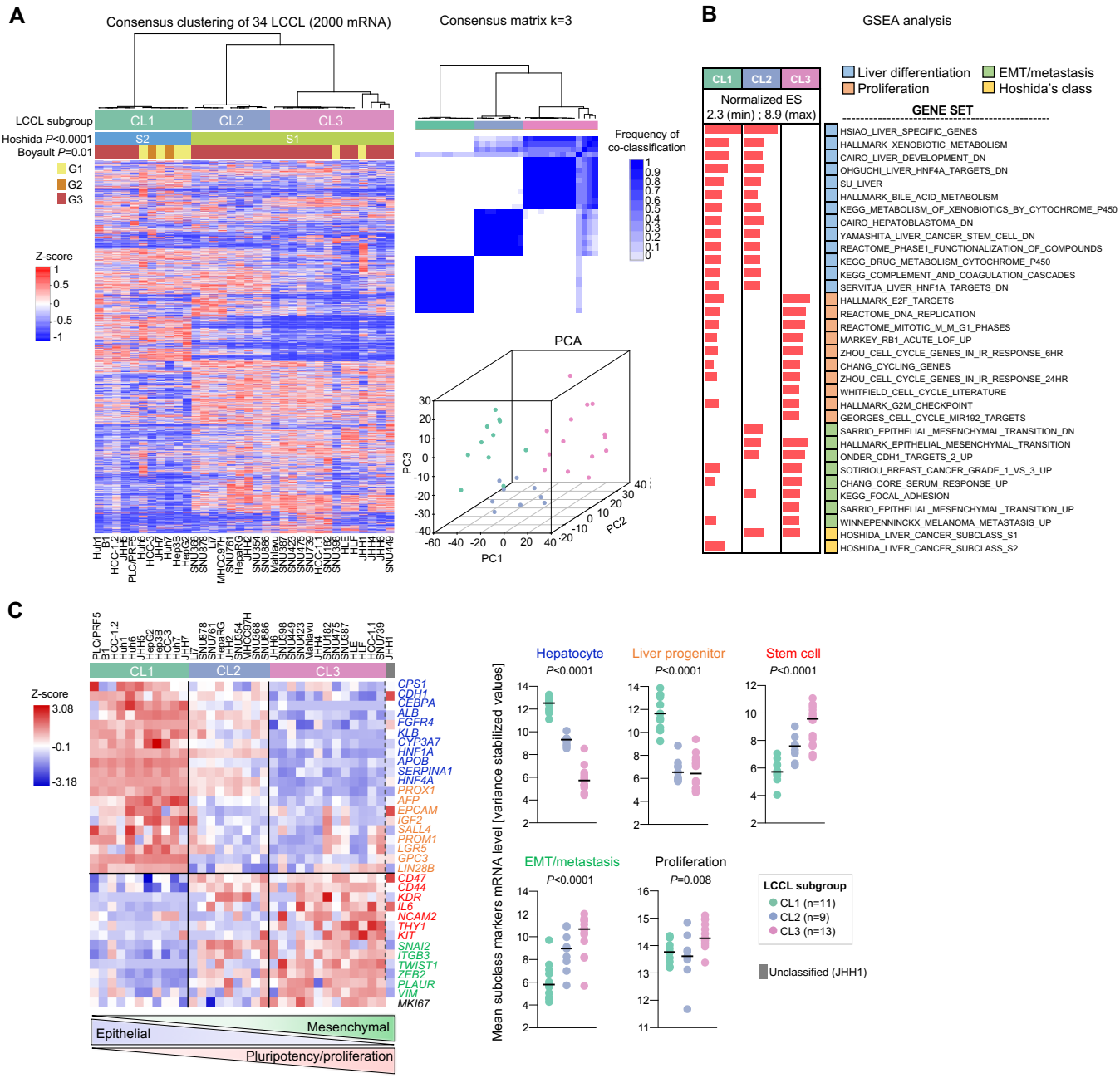
A
Consensus clustering of 34 LCCL (2000 mRNA)
Consensus matrix k=3
LCCL subgroup
CL1
CL2
CL3
Hoshida P<0.0001
S2
S1
Boyault P=0.01
G1
G2
G3
Z-score
Frequency of co-classification
PCA
PC1
PC2
PC3
B
GSEA analysis
Normalized ES
2.3 (min) ; 8.9 (max)
Liver differentiation
Proliferation
EMT/metastasis
Hoshida's class
GENE SET
HSIAO_LIVER_SPECIFIC_GENES
HALLMARK_XENOBIOTIC_METABOLISM
CAIRO_LIVER_DEVELOPMENT_DN
OHGUCHI_LIVER_HNF4A_TARGETS_DN
SU_LIVER
HALLMARK_BILE_ACID_METABOLISM
KEGG_METABOLISM_OF_XENOBIOTICS_BY_CYTOCHROME_P450
CAIRO_HEPATOBLASTOMA_DN
YAMASHITA_LIVER_CANCER_STEM_CELL_DN
REACTOME_PHASE1_FUNCTIONALIZATION_OF_COMPOUNDS
KEGG_DRUG_METABOLISM_CYTOCHROME_P450
KEGG_COMPLEMENT_AND_COAGULATION_CASCADES
SERVITJA_LIVER_HNF1A_TARGETS_DN
HALLMARK_E2F_TARGETS
REACTOME_DNA_REPLICATION
REACTOME_MITOTIC_M_M_G1_PHASES
MARKEY_RB1_ACUTE_LOF_UP
ZHOU_CELL_CYCLE_GENES_IN_IR_RESPONSE_6HR
CHANG_CYCLING_GENES
ZHOU_CELL_CYCLE_GENES_IN_IR_RESPONSE_24HR
WHITFIELD_CELL_CYCLE_LITERATURE
HALLMARK_G2M_CHECKPOINT
GEORGES_CELL_CYCLE_MIR192_TARGETS
SARRIO_EPITHELIAL_MESENCHYMAL_TRANSITION_DN
HALLMARK_EPITHELIAL_MESENCHYMAL_TRANSITION
ONDER_CDH1_TARGETS_2_UP
SOTIRIOU_BREAST_CANCER_GRADE_1_VS_3_UP
CHANG_CORE_SERUM_RESPONSE_UP
KEGG_FOCAL_ADHESION
SARRIO_EPITHELIAL_MESENCHYMAL_TRANSITION_UP
WINNEPENNINCKX_MELANOMA_METASTASIS_UP
HOSHIDA_LIVER_CANCER_SUBCLASS_S1
HOSHIDA_LIVER_CANCER_SUBCLASS_S2
C
Z-score
3.08
-0.1
-3.18
CPS1
CDH1
CEBPA
ALB
FGFR4
KLB
CYP3A7
HNF1A
APOB
SERPINA1
HNF4A
PROX1
AFP
EPCAM
IGF2
SALL4
PROM1
LGR5
GPC3
LIN28B
CD47
CD44
KDR
IL6
NCAM2
THY1
KIT
SNAI2
ITGB3
TWIST1
ZEB2
PLAUR
VIM
MKI67
Epithelial
Mesenchymal
Pluripotency/proliferation
Hepatocyte
Liver progenitor
Stem cell
EMT/metastasis
Proliferation
P<0.0001
P=0.008
Mean subclass markers mRNA level [variance stabilized values]
LCCL subgroup
CL1 (n=11)
CL2 (n=9)
CL3 (n=13)
Unclassified (JHH1)

Figure 3

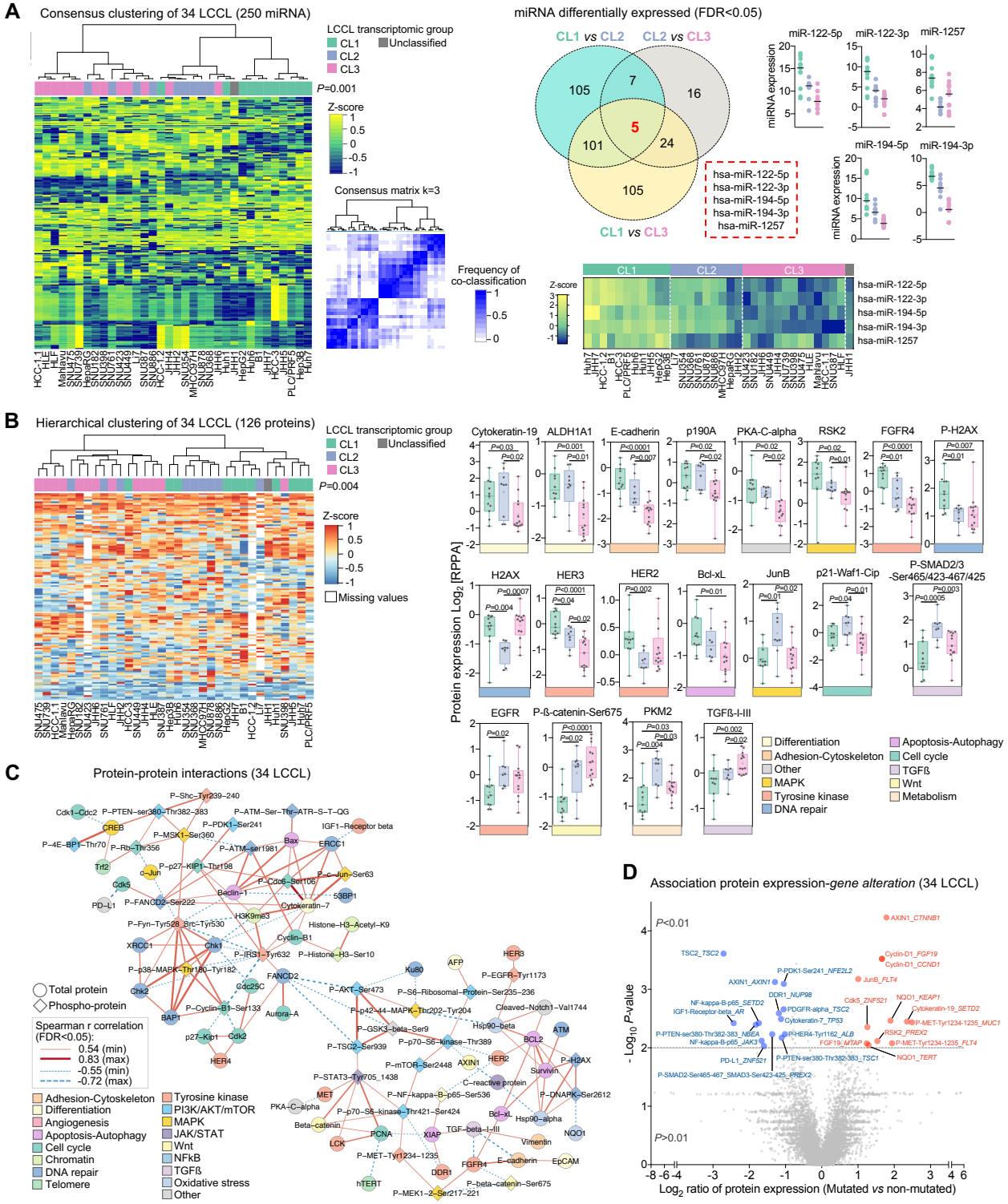
A
Consensus clustering of 34 LCCL (250 miRNA)
LCCL transcriptomic group
CL1
CL2
CL3
Unclassified
P=0.001
Z-score
Consensus matrix k=3
Frequency of co-classification
miRNA differentially expressed (FDR<0.05)
CL1 vs CL2
CL2 vs CL3
CL1 vs CL3
105
7
16
5
101
24
105
hsa-miR-122-5p
hsa-miR-122-3p
hsa-miR-194-5p
hsa-miR-194-3p
hsa-miR-1257
miR-122-5p
miR-122-3p
miR-1257
miR-194-5p
miR-194-3p
miRNA expression
B
Hierarchical clustering of 34 LCCL (126 proteins)
LCCL transcriptomic group
P=0.004
Missing values
Protein expression Log2 [RPPA]
Cytokeratin-19
ALDH1A1
E-cadherin
p190A
PKA-C-alpha
RSK2
FGFR4
P-H2AX
H2AX
HER3
HER2
Bcl-xL
JunB
p21-Waf1-Cip
P-SMAD2/3 -Ser465/423-467/425
EGFR
P-ß-catenin-Ser675
PKM2
TGFß-I-III
Differentiation
Adhesion-Cytoskeleton
Other
MAPK
Tyrosine kinase
DNA repair
Apoptosis-Autophagy
Cell cycle
TGFß
Wnt
Metabolism
C
Protein-protein interactions (34 LCCL)
Total protein
Phospho-protein
Spearman r correlation (FDR<0.05):
0.54 (min)
0.83 (max)
-0.55 (min)
-0.72 (max)
Adhesion-Cytoskeleton
Differentiation
Angiogenesis
Apoptosis-Autophagy
Cell cycle
Chromatin
DNA repair
Telomere
Tyrosine kinase
PI3K/AKT/mTOR
MAPK
JAK/STAT
Wnt
NFkB
TGFß
Oxidative stress
Other
D
Association protein expression-gene alteration (34 LCCL)
P<0.01
P>0.01
- Log10 P-value
Log2 ratio of protein expression (Mutated vs non-mutated)

Figure 4

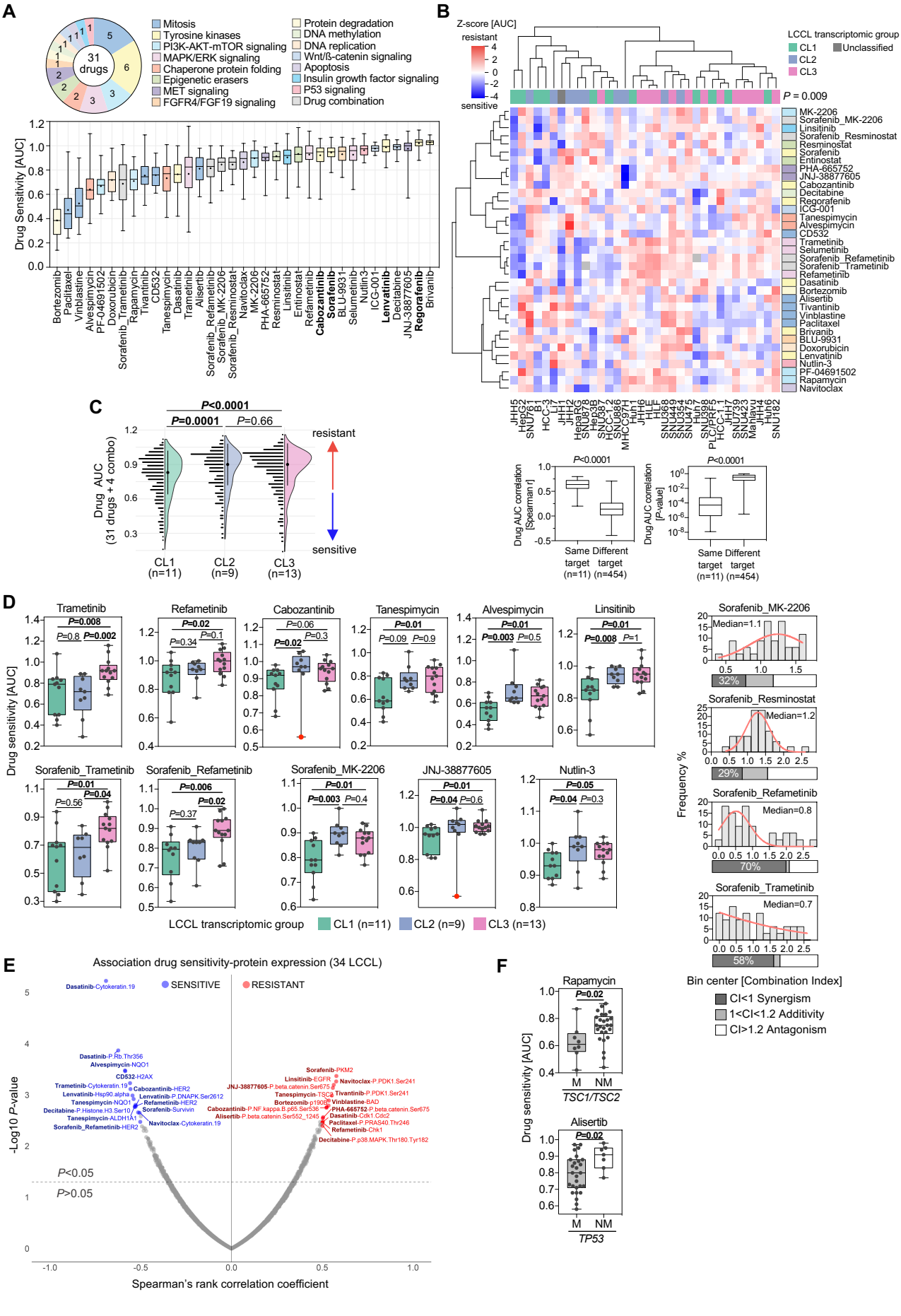
A
31 drugs
Mitosis
Tyrosine kinases
PI3K-AKT-mTOR signaling
MAPK/ERK signaling
Chaperone protein folding
Epigenetic erasers
MET signaling
FGFR4/FGF19 signaling
Protein degradation
DNA methylation
DNA replication
Wnt/ß-catenin signaling
Apoptosis
Insulin growth factor signaling
P53 signaling
Drug combination
Drug Sensitivity [AUC]
Bortezomib
Paclitaxel
Vinblastine
Alvespimycin
PF-04691502
Doxorubicin
Sorafenib_Trametinib
Rapamycin
Tivantinib
CD532
Tanespimycin
Dasatinib
Trametinib
Alisertib
Sorafenib_Refametinib
Sorafenib_MK-2206
Sorafenib_Resminostat
Navitoclax
MK-2206
PHA-665752
Resminostat
Linsitinib
Entinostat
Refametinib
Cabozantinib
Sorafenib
BLU-9931
Selumetinib
Nutlin3
ICG-001
Lenvatinib
Decitabine
JNJ-38877605
Regorafenib
Brivanib
B
Z-score [AUC]
resistant
sensitive
LCCL transcriptomic group
CL1
CL2
CL3
Unclassified
P = 0.009
MK-2206
Sorafenib_MK-2206
Linsitinib
Sorafenib_Resminostat
Resminostat
Sorafenib
Entinostat
PHA-665752
JNJ-38877605
Cabozantinib
Decitabine
Regorafenib
ICG-001
Tanespimycin
Alvespimycin
CD532
Trametinib
Selumetinib
Sorafenib_Refametinib
Sorafenib_Trametinib
Refametinib
Dasatinib
Bortezomib
Alisertib
Tivantinib
Vinblastine
Paclitaxel
Brivanib
BLU-9931
Doxorubicin
Lenvatinib
Nutlin-3
PF-04691502
Rapamycin
Navitoclax
JHH5
HepG2
SNU761
B1
HCC-3
JHH1
JHH2
HepaRG
SNU878
SNU387
HCC-1-2
SNU886
MHCC97H
JHH7
JHH6
HLE
HLF
SNU398
SNU449
SNU354
SNU475
Huh7
SNU368
PLC-PRF-5
HCC-1-1
JHH13
JHH7
SNU739
SNU423
Mahlavu
JHH4
Huh6
SNU182
P<0.0001
Drug AUC correlation [Spearman r]
Same target (n=11)
Different target (n=454)
P<0.0001
Drug AUC correlation [P-value]
Same target (n=11)
Different target (n=454)
C
P<0.0001
P=0.0001
P=0.66
Drug AUC (31 drugs + 4 combo)
resistant
sensitive
CL1 (n=11)
CL2 (n=9)
CL3 (n=13)
D
Trametinib
Refametinib
Cabozantinib
Tanespimycin
Alvespimycin
Linsitinib
Drug sensitivity [AUC]
Sorafenib_Trametinib
Sorafenib_Refametinib
Sorafenib_MK-2206
JNJ-38877605
Nutlin-3
LCCL transcriptomic group
CL1 (n=11)
CL2 (n=9)
CL3 (n=13)
Sorafenib_MK-2206
Median=1.1
32%
Sorafenib_Resminostat
Median=1.2
29%
Sorafenib_Refametinib
Median=0.8
70%
Sorafenib_Trametinib
Median=0.7
58%
Frequency %
Bin center [Combination Index]
CI<1 Synergism
1<CI<1.2 Additivity
CI>1.2 Antagonism
E
Association drug sensitivity-protein expression (34 LCCL)
SENSITIVE
RESISTANT
-Log10 P-value
P<0.05
P>0.05
Spearman's rank correlation coefficient
F
Rapamycin
Drug sensitivity [AUC]
M
NM
TSC1/TSC2
Alisertib
M
NM
TP53

Figure 5

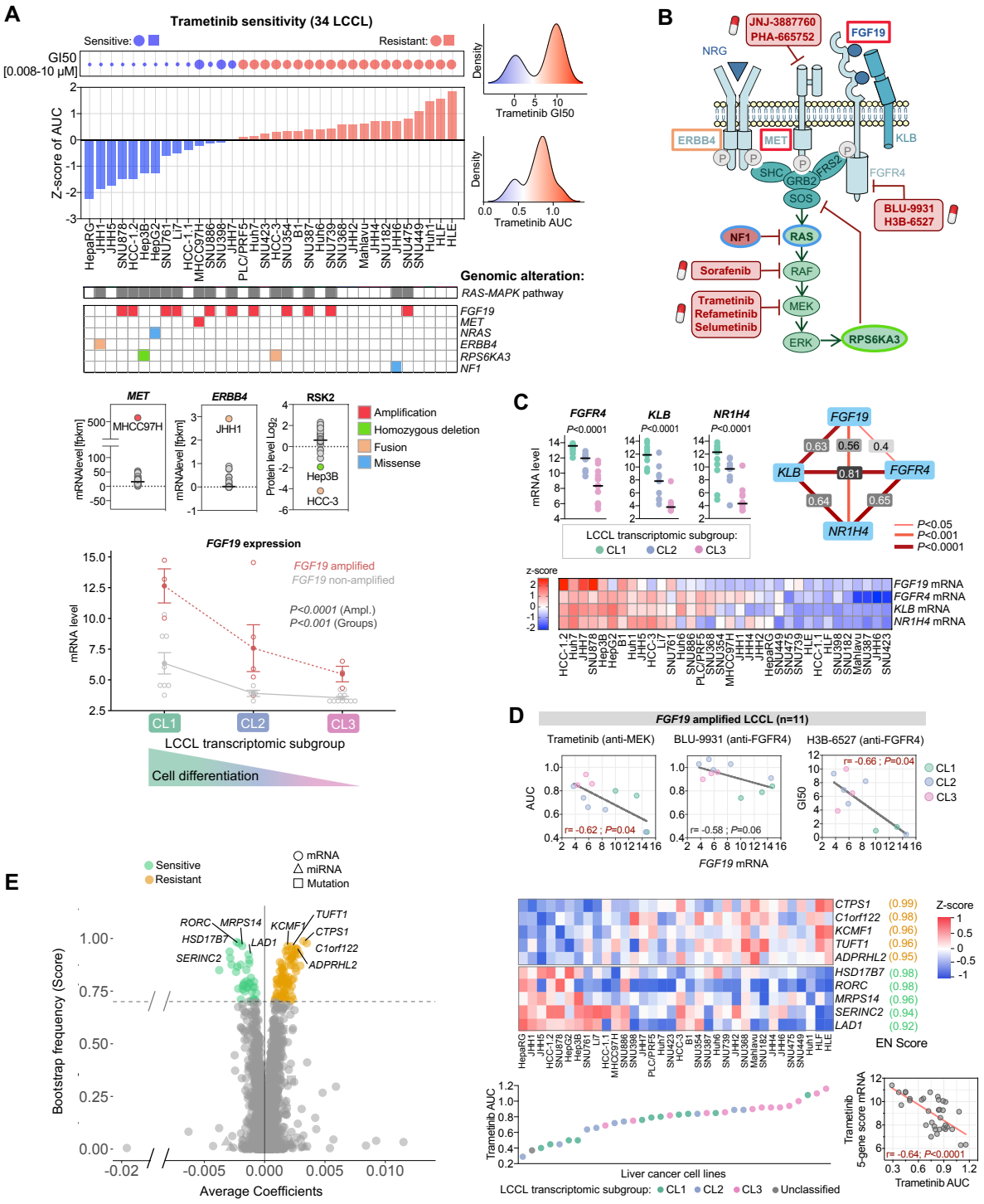
A
Trametinib sensitivity (34 LCCL)
Sensitive:
Resistant:
GI50 [0.008-10 μM]
Z-score of AUC
Density
Trametinib GI50
Trametinib AUC
HepaRG JHH1 JHH5 SNU878 HCC-1.2 Hep3B HepG2 SNU761 LI7 HCC-1.1 MHCC97H SNU886 SNU398 JHH7 PLC/PRF5 Huh7 SNU423 HCC-3 SNU354 B1 SNU387 Huh6 SNU739 SNU368 JHH2 Mahlavu JHH4 SNU182 JHH6 SNU475 SNU449 Huh1 HLF HLE
Genomic alteration:
RAS-MAPK pathway
FGF19
MET
NRAS
ERBB4
RPS6KA3
NF1
MET
ERBB4
RSK2
mRNAlevel [fpkm]
Protein level Log2
MHCC97H
JHH1
Hep3B
HCC-3
Amplification
Homozygous deletion
Fusion
Missense
FGF19 expression
FGF19 amplified
FGF19 non-amplified
P<0.0001 (Ampl.)
P<0.001 (Groups)
mRNA level
CL1
CL2
CL3
LCCL transcriptomic subgroup
Cell differentiation
B
JNJ-3887760
PHA-665752
FGF19
NRG
ERBB4
MET
KLB
FGFR4
SHC
GRB2
FRS2
SOS
BLU-9931
H3B-6527
NF1
RAS
Sorafenib
RAF
Trametinib
Refametinib
Selumetinib
MEK
ERK
RPS6KA3
C
FGFR4
KLB
NR1H4
P<0.0001
mRNA level
LCCL transcriptomic subgroup:
CL1 CL2 CL3
FGF19
KLB
FGFR4
NR1H4
0.63
0.56
0.4
0.81
0.64
0.65
P<0.05
P<0.001
P<0.0001
z-score
FGF19 mRNA
FGFR4 mRNA
KLB mRNA
NR1H4 mRNA
D
FGF19 amplified LCCL (n=11)
Trametinib (anti-MEK)
BLU-9931 (anti-FGFR4)
H3B-6527 (anti-FGFR4)
AUC
GI50
r= -0.62 ; P=0.04
r= -0.58 ; P=0.06
r= -0.66 ; P=0.04
FGF19 mRNA
CL1
CL2
CL3
E
Sensitive
Resistant
mRNA
miRNA
Mutation
Bootstrap frequency (Score)
Average Coefficients
RORC
MRPS14
HSD17B7
LAD1
SERINC2
KCMF1
TUFT1
CTPS1
C1orf122
ADPRHL2
CTPS1 (0.99)
C1orf122 (0.98)
KCMF1 (0.96)
TUFT1 (0.96)
ADPRHL2 (0.95)
HSD17B7 (0.98)
RORC (0.98)
MRPS14 (0.96)
SERINC2 (0.94)
LAD1 (0.92)
Z-score
EN Score
Trametinib AUC
Liver cancer cell lines
LCCL transcriptomic subgroup: CL1 CL2 CL3 Unclassified
Trametinib 5-gene score mRNA
r= -0.64; P<0.0001
Trametinib AUC

Figure 6

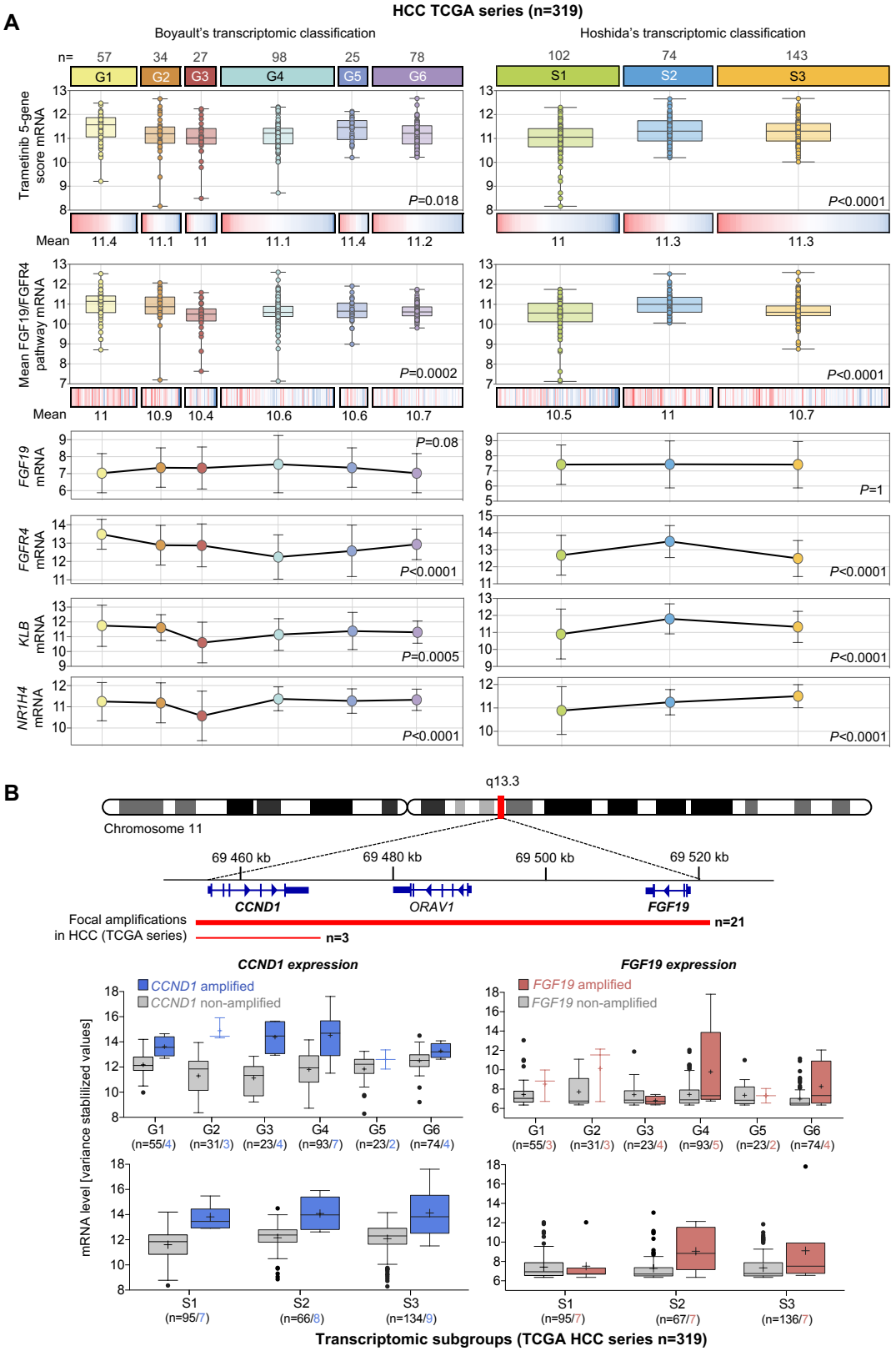
A
HCC TCGA series (n=319)
Boyault's transcriptomic classification
Hoshida's transcriptomic classification
n= 57 34 27 98 25 78
G1 G2 G3 G4 G5 G6
102 74 143
S1 S2 S3
Trametinib 5-gene score mRNA
P=0.018
P<0.0001
Mean 11.4 11.1 11 11.1 11.4 11.2
11 11.3 11.3
Mean FGF19/FGFR4 pathway mRNA
P=0.0002
P<0.0001
Mean 11 10.9 10.4 10.6 10.6 10.7
10.5 11 10.7
FGF19 mRNA
P=0.08
P=1
FGFR4 mRNA
P<0.0001
P<0.0001
KLB mRNA
P=0.0005
P<0.0001
NR1H4 mRNA
P<0.0001
P<0.0001
B
q13.3
Chromosome 11
69 460 kb
69 480 kb
69 500 kb
69 520 kb
CCND1
ORAV1
FGF19
Focal amplifications in HCC (TCGA series)
n=21
n=3
CCND1 expression
FGF19 expression
CCND1 amplified
CCND1 non-amplified
FGF19 amplified
FGF19 non-amplified
mRNA level [variance stabilized values]
G1 (n=55/4) G2 (n=31/3) G3 (n=23/4) G4 (n=93/7) G5 (n=23/2) G6 (n=74/4)
G1 (n=55/3) G2 (n=31/3) G3 (n=23/4) G4 (n=93/5) G5 (n=23/2) G6 (n=74/4)
S1 (n=95/7) S2 (n=66/8) S3 (n=134/9)
S1 (n=95/7) S2 (n=67/7) S3 (n=136/7)
Transcriptomic subgroups (TCGA HCC series n=319)

Figure 7

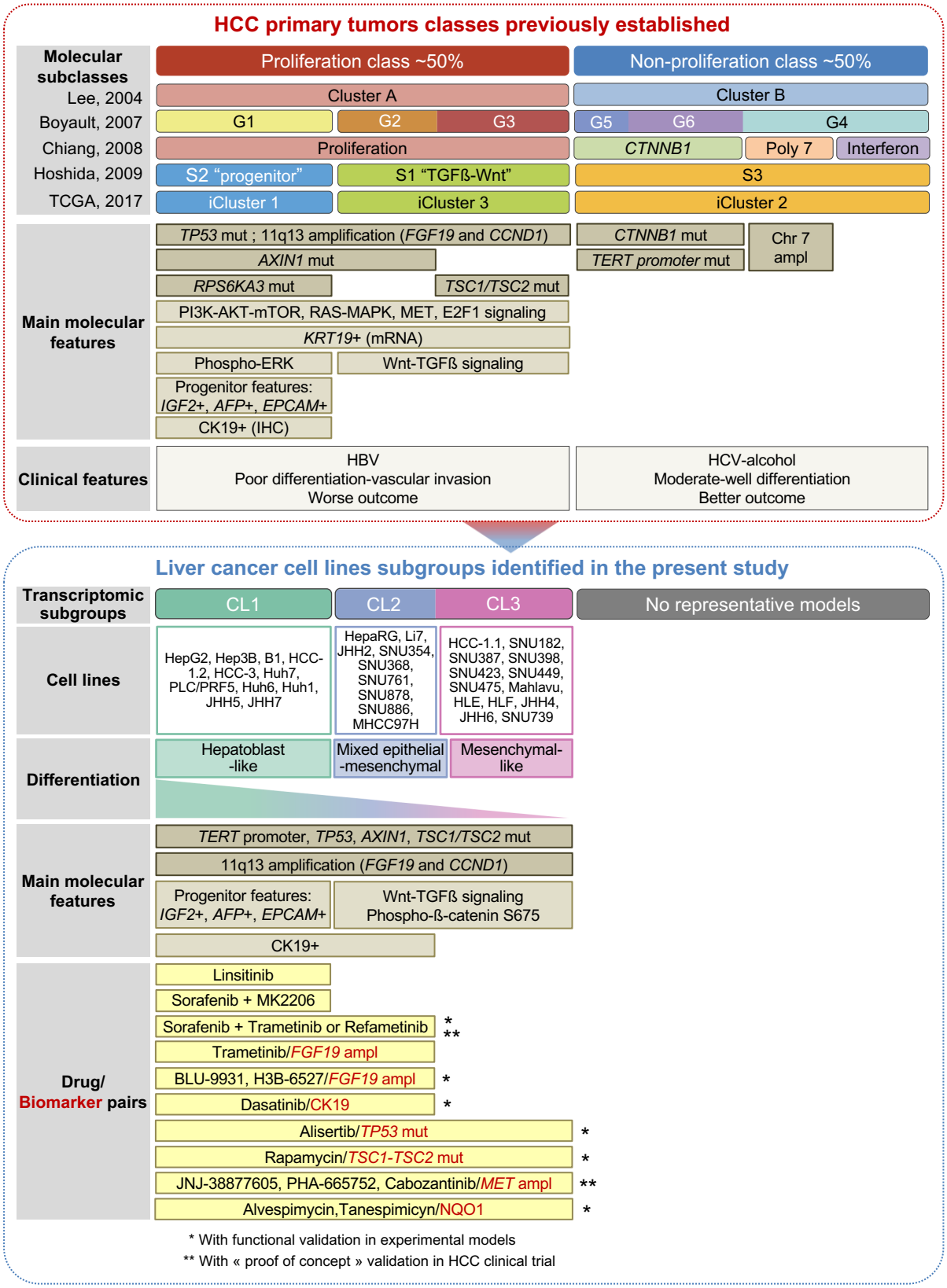
HCC primary tumors classes previously established
Molecular subclasses
Proliferation class ~50%
Non-proliferation class ~50%
Lee, 2004
Cluster A
Cluster B
Boyault, 2007
G1
G2
G3
G5
G6
G4
Chiang, 2008
Proliferation
CTNNB1
Poly 7
Interferon
Hoshida, 2009
S2 "progenitor"
S1 "TGFß-Wnt"
S3
TCGA, 2017
iCluster 1
iCluster 3
iCluster 2
Main molecular features
TP53 mut ; 11q13 amplification (FGF19 and CCND1)
CTNNB1 mut
TERT promoter mut
Chr 7 ampl
AXIN1 mut
RPS6KA3 mut
TSC1/TSC2 mut
PI3K-AKT-mTOR, RAS-MAPK, MET, E2F1 signaling
KRT19+ (mRNA)
Phospho-ERK
Wnt-TGFß signaling
Progenitor features: IGF2+, AFP+, EPCAM+
CK19+ (IHC)
Clinical features
HBV
Poor differentiation-vascular invasion
Worse outcome
HCV-alcohol
Moderate-well differentiation
Better outcome
Liver cancer cell lines subgroups identified in the present study
Transcriptomic subgroups
CL1
CL2
CL3
No representative models
Cell lines
HepG2, Hep3B, B1, HCC-1.2, HCC-3, Huh7, PLC/PRF5, Huh6, Huh1, JHH5, JHH7
HepaRG, Li7, JHH2, SNU354, SNU368, SNU761, SNU878, SNU886, MHCC97H
HCC-1.1, SNU182, SNU387, SNU398, SNU423, SNU449, SNU475, Mahlavu, HLE, HLF, JHH4, JHH6, SNU739
Differentiation
Hepatoblast -like
Mixed epithelial -mesenchymal
Mesenchymal-like
Main molecular features
TERT promoter, TP53, AXIN1, TSC1/TSC2 mut
11q13 amplification (FGF19 and CCND1)
Progenitor features: IGF2+, AFP+, EPCAM+
Wnt-TGFß signaling
Phospho-ß-catenin S675
CK19+
Drug/ Biomarker pairs
Linsitinib
Sorafenib + MK2206
Sorafenib + Trametinib or Refametinib
*
**
Trametinib/FGF19 ampl
BLU-9931, H3B-6527/FGF19 ampl
*
Dasatinib/CK19
*
Alisertib/TP53 mut
*
Rapamycin/TSC1-TSC2 mut
*
JNJ-38877605, PHA-665752, Cabozantinib/MET ampl
**
Alvespimycin,Tanespimicyn/NQO1
*
* With functional validation in experimental models
** With « proof of concept » validation in HCC clinical trial